ARCHIVES OF METALLURGY AND MATERIALS
Volume 51 2006 Issue 4

D. PODORSKA*, P. DROŻDŻ*, J. FALKUS*, J. WYPARTOWICZ*

CALCULATIONS OF OXIDE INCLUSIONS COMPOSITION IN THE STEEL DEOXIDIZED WITH Mn, Si AND Ti

OBLICZANIE SKŁADU WYDZIELEŃ TLENKOWYCH W STALI ODTLENIANEJ PRZY POMOCY Mn, Si I Ti

The work deals with the determination of the composition of liquid oxide solution MnO-SiO_2-TiO_2-Al_2O_3, present as an inclusion in liquid steel during its solidification. The region of compositions at which oxide solution remains entirely liquid at the temperatures 1523 K and 1673 was calculated by means of FACT program. The evolution of oxide phase chemical composition in thermodynamic equilibrium with liquid steel during its equilibrium solidification was calculated. The procedure of calculations may be applied in the determination of the conditions for acicular ferrite formation, which nucleates at oxide inclusions.

***Keywords*: steel, solidification, oxide inclusions, thermodynamic equilibrium, acicular ferrite**

Praca zajmuje się określeniem zmian składu ciekłego roztworu tlenkowego MnO-SiO_2-TiO_2-Al_2O_3 znajdującego się w postaci wtrącenia w ciekłej stali w trakcie jej krzepnięcia. Obliczono przy pomocy programu FACT zakres składów roztworu tlenkowego, przy jakim pozostaje on całkowicie ciekły przy temperaturach 1523 i 1673 K. Wyznaczono ewolucję składu chemicznego fazy tlenkowej pozostającej w równowadze termodynamicznej z ciekłą stalą w trakcie jej równowagowego krzepnięcia. Procedura obliczeniowa może być zastosowana do określania warunków tworzenia ferrytu iglastego zarodkującego na wydzieleniach tlenkowych.

1. Introduction

Promotion of acicular ferrite formation in low alloyed low carbon steel due to the presence of fine oxide inclusions is a spectacular example of so called “oxide metallurgy”. Structure termed “acicular ferrite” is composed of the clusters of needle-shaped ferrite grains, about 30 μm long. Neighbouring grains in clusters differ in orientation, what results in better ability to interlock the cracks, what results in better mechanical properties of steel [1-4]. Ishikawa et al [1] confirmed experimentally that such structure may be obtained even from large austenite grains, what is the case in welding operations, where austenite grains grow strongly in the heat affected zone.

To obtain such structure, the heterogeneous nucleation centres, i.e. non-metallic inclusions must be present in the austenite grains. Gregg and Bhadeshia [2] demonstrated experimentally that various compounds as CuS, TiN or γ-Al_2O_3 may be active in acicular ferrite formation. However in common steelmaking practice the simplest possibility consists in employing oxide solution based on MnO-SiO_2-TiO_2 system. The necessary conditions of favourable action of inclusions are their similar dimensions of the order 1 μm and even distribution in steel. This may be achieved only if the inclusions form and transform during the solidification of steel. For this reason aluminium cannot be used as main steel deoxidizer, as approximately 50 ppm of oxygen is needed in steel to form secondary inclusions for the purpose of acicular ferrite nucleation. Thus primary deoxidization has to be carried out mainly with silicon and manganese.

Another important reason of application of manganese and silicon, and also some amount of titanium, results from the mode of acicular ferrite formation. Shim et al [4] and Kim et al [5] have shown experimentally by means of X-ray microanalysis that around the inclusions based on titanium oxide the manganese depleted zone of the radius 10-35 μm is formed. In the close vicinity of inclusion the manganese concentration is very low, even if its average concentration in steel is about 1.5% [4]. This zone formation is a result of

---

* FACULTY OF METALS ENGINEERING AND INDUSTRIAL INFORMATICS, AGH - UNIVERSITY OF SCIENCE AND TECHNOLOGY, 30-059 KRAKÓW, 30 MICKIEWICZA AVE., POLAND

manganese transfer to the inclusion and its absorption. Gregg and Bhadeshia [2] point out that similar effect of carbon depletion appears under the influence of titanium oxide present in inclusion, whereas the local changes in silicon concentration were not observed. Manganese is the austenite stabilizing element, so its local deficiency results in ferrite appearance. The difference of manganese concentration may be counted as the driving force of ferrite crystallization.

It is so far not clear, how manganese is bonded in non-metallic inclusion. Several authors found experimentally, that manganese is present in inclusion in the form of MnS (e.g. Kim et al [5], Oikawa et al [6], Ohta et al [7]. As the average sulphur content in steel is within the range 0.005% – 0.01%, during crystallization MnS is formed together with small amount of FeS. It results from high manganese affinity to sulphur that MnS appears in the inclusions, which are mainly consisted of oxide solution. At the cooling rate 50 K/min the dimensions of these inclusions are about 3 μm, while at the cooling rate 500 K/min the inclusion dimensions below 1 μm may be obtained. The range of cooling rates 50-500 K/min is typical for the conditions of continuous casting. The prevailing part of inclusions observed in steel ingot has mixed character. It consists of oxide part and smaller fragment of MnS [5, 6]. Typical inclusions contain one or two substantial fragments of MnS; the inclusions with MnS envelope are rather sporadic. These two types of inclusions constitute 90% of whole population at the concentration of sulphur about 150 ppm. The inclusions of pure MnS are rare.

The experimental results of Shim et al [2] show that in the sample of synthetic steel, in which sulphur is not present, the manganese depleted zone is also visible around the inclusion, and the acicular ferrite is observed in this zone. Ti_2O_3 contains considerable amount of cation vacancies, which may be occupied by Mn^{2+} cations. Gregg and Bhadeshia [2] investigated the action of synthetic oxide phases and found that the ferritic structure of highest fragmentation is obtained with the use of pure titanium oxides, both TiO_2 and Ti_2O_3. In real process, however, the oxide solution is always present and application of pure oxides is impossible. The pulverized solid oxide introduced into the steel would float and react with the top slag. Uniform distribution of inclusions is only possible if they precipitate from liquid steel close to the freezing front. The MnO-TiO_2 solution has too high melting temperature, so third oxide component is needed. Silicon oxide is more suitable, as it allows for better oxygen control.

It is suggested [2] that the action of inclusions consists not only in absorption of manganese from surroundings, but also in creation the strains on cooling, which may be discharged in the austenite transition into ferrite. These strains are created due to the large difference between the thermal expansion coefficients of steel and oxide. Madariaga et al [3] emphasize the role of thin layer of CuS on the surface of MnS. They suggest that that large difference in lattice parameters between face centered austenite and hexagonal CuS initiates the precipitation of ferrite. It is also possible that the difference between austenite-sulphide and ferrite-sulphide surface energies is the result of difference in lattice parameters.

Most of the above presented mechanisms of magnesium depleted zones require the oxide inclusion to remain liquid in solid steel down to temperatures approximately 1200°C. This may be achieved if the oxide inclusion is composed of MnO, SiO_2 and TiO_2. Some amount of Al is also present in steel, what results in the presence of Al_2O_3 in liquid oxide. The present work is an attempt to find the means of control of oxide inclusion composition on the basis of the initial composition of steel. Two questions have to be answered: what is the region of liquid phase in the system MnO-SiO_2-TiO_2-Al_2O_3 at the temperatures below the solidus of steel, and how the oxide composition varies in the course of steel solidification.

2. Calculation of liquid region in the MnO-SiO_2-TiO_2-Al_2O_3 system

The determination of liquid region in the MnO-SiO_2-TiO_2 and MnO-SiO_2-TiO_2-Al_2O_3 systems was carried out with the use of FACT software for thermodynamic calculations. The fraction of solid phase f_s was calculated along the Gibbs triangle sections of constant TiO_2 molar fraction. The applied intervals of TiO_2 content were 0.01 (mole fraction). The points for which $f_S = 0$ were then converted into the lines, delineating liquid phase range. The liquid phase range in ternary system MnO-SiO_2-TiO_2 obtained in the present work is presented in Fig. 1. The liquid phase area for the temperature 1673 K is very close to this obtained by Ohta et al [7]. At the temperature 1523 the liquid phase area is strongly reduced. The liquid range in the quaternary system MnO-SiO_2-TiO_2-Al_2O_3 was not reported in the literature. The results of calculations are presented in Figs 2–4 in the form of the isothermal sections at the molar fraction of Al_2O_3 equal to 0.05, 0.10 and 0.15. It is clear that the liquid phase range is wide at the compositions close to MnO-SiO_2 binary system. Addition of Al_2O_3 results in considerable increase of liquid phase field in the region of compositions close to binary MnO-SiO_2.

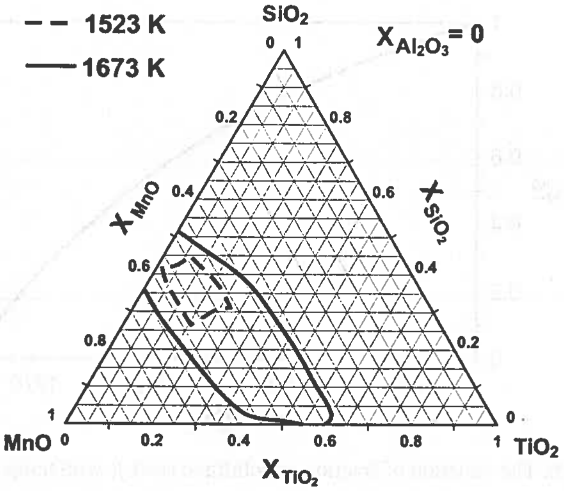

Fig. 1. Calculated region of liquid phase in MnO-SiO_2-TiO_2 system at 1523 and 1673 K

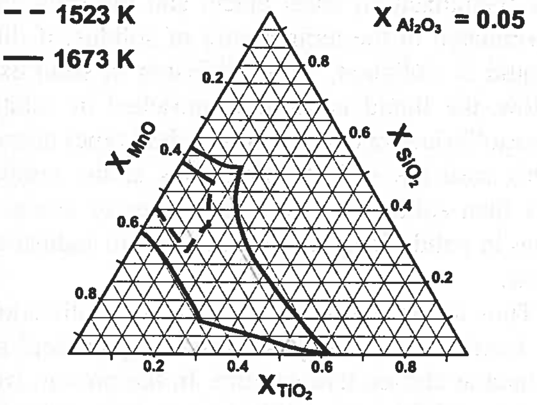

Fig. 2. Calculated region of liquid phase in MnO-SiO_2-TiO_2-Al_2O_3 system at 1523 and 1673 K at Al_2O_3 concentration 0.05 (mole fraction)

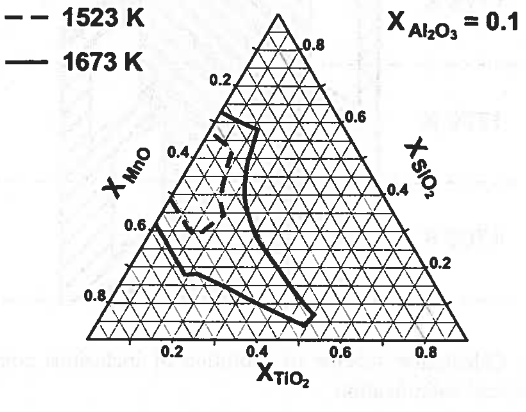

Fig. 3. Calculated region of liquid phase in MnO-SiO_2-TiO_2-Al_2O_3 system at 1523 and 1673 K at Al_2O_3 concentration 0.1 (mole fraction)

multicols

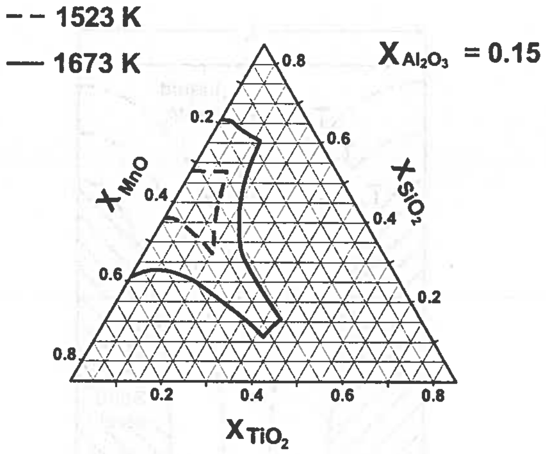

Fig. 4. Calculated region of liquid phase in MnO-SiO_2-TiO_2-Al_2O_3 system at 1523 and 1673 K at Al_2O_3 concentration 0.15 (mole fraction)

3. Calculation of phase compositions during steel solidification

At the temperatures above liquidus of steel two-phase equilibrium between liquid steel and liquid oxide solution has to be considered. At the temperatures below liquidus three phases are present: liquid steel, solid steel and liquid oxide solution. However, full thermodynamic equilibrium between three phases usually cannot be reached in such case. This is mainly due to the very limited possibility of mass exchange between solid steel and liquid oxide phase.

The thermodynamic equilibrium between liquid and solid steel during solidification of multi-component solution is governed by two main factors: initial steel composition and the cooling rate. In real industrial process, even in stationary regime, the cooling rate varies between different sites in the ingot.

The simulations in the present work were carried out under assumption of dendritic growth. Small volume of liquid is considered, in which the solid phase appears and grows. It should be noticed that such solidification model prevents the coalescence of inclusions. Scheme of diagonal section of such elementary volume is presented in Fig. 5. The size of elementary volume is determined through the distance between axes of secondary dendrite arms λ, which is represented by the empirical dependence on the cooling rate [8]:

$$\lambda(\mu m) = 688 \cdot (dT/dt)^{-0.36}, \qquad (1)$$

where dT/dt (K/min) denotes the cooling rate.

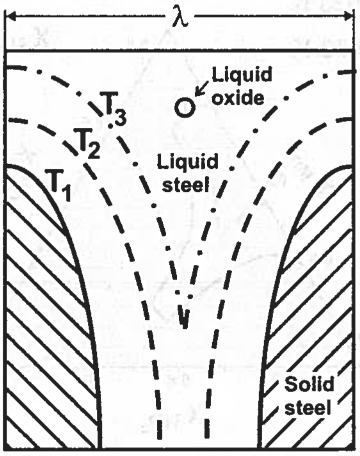

Fig. 5. Scheme of the cell corresponding to single oxide inclusion formation ($T_1 > T_2 > T_3$)

The relation for progress of solidification, i.e. between the temperature and the fraction of solid phase was assumed according to Ma and Janke [8] as:

$$f_S = \frac{T_L - T}{T_0 - T} \cdot \frac{T_0 - T_S}{T_L - T_S}, \tag{2}$$

where: T – temperature at given stage of solidification f_S, $T_0 = 1809K$ – melting point of pure iron, T_L – liquidus temperature of steel, T_S – solidus temperature of steel.

The composition of steel under consideration is given in table I.

TABLE

The initial composition of liquid steel (including oxide phase)

Steel component	C	Si	Mn	Al	Ti	O
Concentration	0.04%	0.17%	0.74%	3 ppm	30 ppm	50 ppm

Liquidus temperature of this steel was calculated from relation (3), according to [9]:

$$T_L = 1809 - \{100.3 \cdot [\%C] - 22.4 \cdot [\%C]^2 + 13.55 \cdot [\%Si] - 0.64 \cdot [\%Si]^2 + 5.82 \cdot [\%Mn] + 0.3 \cdot [\%Mn]^2 . \tag{3}$$

The resulting value is $T_L = 1775K$. The solidus temperature was arbitrarily assumed as $T_S = 1735K$. The dependence of solid phase fraction on temperature is shown in Fig. 6. Distribution of steel components between solid and liquid phase is governed by the mode of crystallization. It is a result of two processes:

- Increase of concentration of liquid steel components due to their segregation at the front of solidification,
- Decrease of their concentration in liquid due to back diffusion into solid phase.

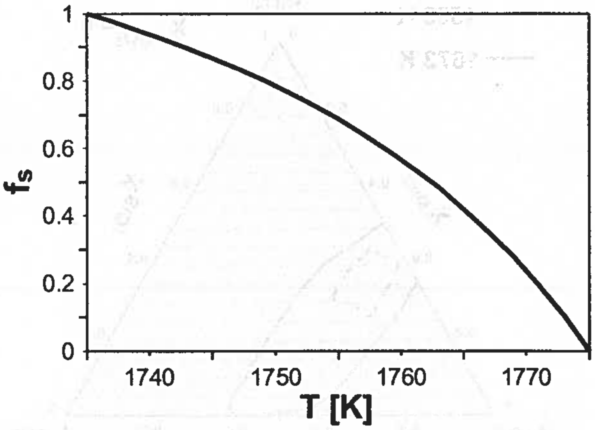

Fig. 6. The variation of fraction of solidified steel f_s with temperature

From this point of view two limiting cases of crystallization may be considered. Under assumption of sufficiently quick (in comparison to the crystallization rate) diffusion in both solid and liquid phases the equilibrium crystallization takes place, and the crystallization is terminated in the temperature of solidus. If diffusion in liquid is sufficient, while diffusion in solid extremely slow, the liquid is strongly enriched in solutes and non-equilibrium crystallization (Scheil type) takes place. In this case the solidification ends at the temperature lower than solidus. Intermediate cases of non-zero diffusion in solid phase are usually met in industrial conditions.

Thus according to the mode of crystallization, various fractions and compositions of liquid steel may be obtained at chosen temperature. In the present work the case of equilibrium crystallization is taken into account.

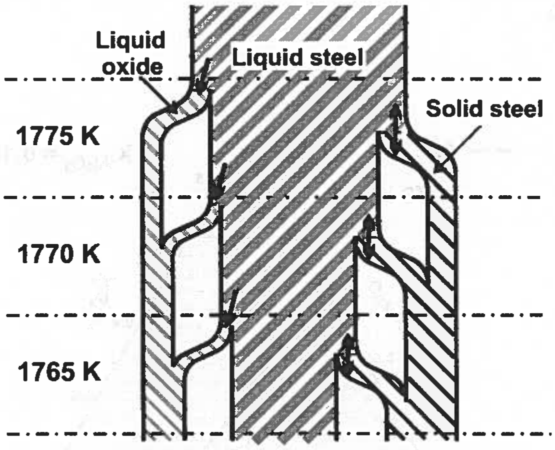

Fig. 7. Calculation scheme of evolution of inclusions composition during steel solidification

Calculation scheme employed in the present work is presented in Fig. 7. At the temperature 1775 K, i.e. at the liquidus temperature, only liquid steel and liquid oxide phase are present. The distribution of components between these phases was calculated by means of simple program, which for given masses of system components yields the amounts and compositions of both phases. Program solves the set of equations, which regards:

- The activities of components in liquid metallic phase, described by means of Wagner-Chipman equations;
- The temperature dependent activities of oxides: MnO, SiO_2, Al_2O_3 and TiO_2 in liquid oxide phase, expressed by regular solution model;
- The temperature dependent equilibrium constants of reactions between metallic components and dissolved oxygen, e.g. $\underline{Mn} + \underline{O} = (MnO)$.

The values of parameters in solution models as well as the equilibrium constants employed in calculations were presented in the paper [10].

As it is seen in Fig. 7, obtained amount of oxide phase at 1775 K is excluded from further calculations of equilibrium. The reason is that the mass exchange between oxide particle and liquid steel is much slower than the solidification rate. In the next step, regarding the temperature 1770 K, new equilibrium is established between the liquid and oxide phase, and the oxide portion is again excluded from equilibrium calculations and added to oxide already present. Then the amounts of components in solid phase are calculated according to the formula:

$$m_i(s) = m_i(l) \cdot \frac{k \cdot f_S}{1 - f_S + k \cdot f_S}, \tag{4}$$

where:

$m_i(s)$ – mass of component "i" in solid phase,

$m_i(l)$ – mass of component "i" in liquid phase prior to separation the portion of solid phase.

As the equilibrium solidification was assumed, the solid metallic phase exchanges components with liquid phase at each calculation step. This is not the case with liquid oxide phase.

The results of calculations are presented in the Figs. 8 and 9. Fig. 8 presents the dependence of the mass of components in solid and liquid phases in the system of total mass 10^6 g. Fig. 8a presents the mass of Mn, Si and total mass of solutes. Fig. 8b presents the mass of Ti and O. Fig 8c shows the mass of Al. It may be noticed, that amounts of all components except aluminum and oxygen in solid steel after full solidification are only slightly smaller in comparison to their initial amounts in the liquid steel. In the case of aluminum it may be noticed that approx. 80% of its initial amount overpasses to oxide phase. In the case of oxygen approx. 60% of initial value moves to liquid oxide. The evolution of composition of liquid oxide phase during crystallization is presented in Fig. 9. It may be observed that the concentration of MnO decreases, while the amount of SiO_2 increases during solidification. The concentrations of Al_2O_3 and TiO_2 slightly decrease. The total mass of oxide inclusions in the case under consideration changes from 54.9 g to 70.8 g (for 1 Mg of steel).

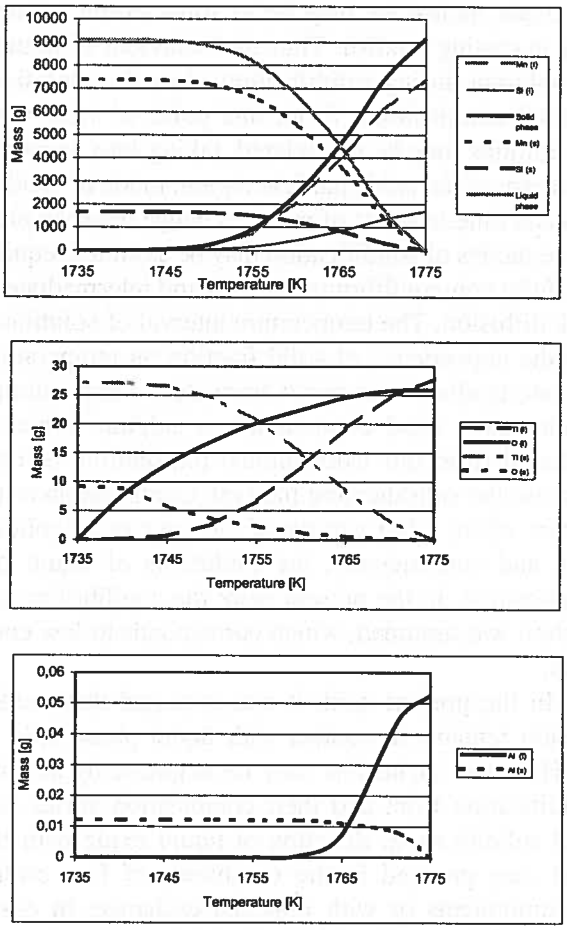

Fig. 8. The evolution of amount of components in solid and liquid steel during solidification (for 1 Mg initial steel amount): a) Mass of Mn, Si and total mass of solutes, b) Mass of Ti and O, c) Mass of Al

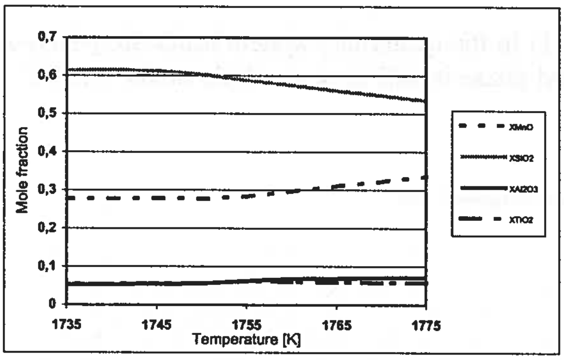

Fig. 9. The change of liquid oxide phase composition during steel solidification

4. Discussion

The proper action of oxide inclusions in acicular ferrite formation requires the oxide phase to be liquid, or at least partly liquid, at the temperature about 1200°C. The composition of liquid steel and, consequently, existing oxide inclusions may be to some extent controlled only in casting tundish. Thus the behaviour of liquid oxide solution during solidification of steel is decisive for its final composition. From this point of view various possibilities may be considered, taking into account the geometry of the oxide particle region, mode of solidification and kinetic terms of mass exchange between phases. Three modes of solidification may be assumed: equilibrium, fully non-equilibrium (Scheil) and intermediate with back diffusion. The temperature interval of solidification and the dependence of solid fraction on temperature in the intermediate case result from steel composition and cooling rate. Steel components as sulphur (which was excluded from our calculations) phosphorus or carbon increase the solidification interval. Combination of these factors offers a big variety of the courses of solidification, and consequently, the evolutions of liquid phase composition. In the present work the equilibrium solidification was assumed, which corresponds to low cooling rates.

In the present work it was assumed that oxide inclusion remains in contact with liquid phase only (Fig. 5). However, inclusions may be engulfed by advancing solidification front and their composition varies during steel solidification. Reaction of liquid oxide with liquid steel may proceed in the conditions of free exchange of components or with impeded exchange. In our calculations the asymmetric components exchange was assumed: free from liquid steel to liquid oxide and lack of transfer in opposite direction.

5. Conclusions

1) In the quaternary system MnO-SiO_2-TiO_2-Al_2O_3 liquid phase is still present a little below 1200°C.

2) The result of calculation of the composition of liquid oxide phase in steel during crystallization is strongly influenced by the crystallization mode, geometric conditions of the inclusion region and the conditions of mass exchange between phases.

3) Initial aluminium concentration in steel at the onset of solidification should be very low. Otherwise the Al_2O_3 concentration in inclusion becomes high and the inclusion solidifies simultaneously with steel.

4) During equilibrium crystallization of steel the composition of liquid phase does not change considerably.

5) The increase of SiO_2 concentration in oxide solution at the cost of MnO results in the increase of its solidification temperature.

Received: 20 September 2006.

Acknowledgements

This work was financed by the Polish Ministry of Education and Science – contract nr 11.11.110.659 (AGH-UST Kraków).

REFERENCES

[1] F. Ishikawa, T. Takahashi, T. Ochi, Met. Mater. Trans. A **25A**, 929-936 (1994).
[2] J. M. Gregg, H. K. Bhadeshia, Acta Mater. **45**, 739-748 (1997).
[3] I. Madriaga, J. L. Romero, I. Gutiérrez, Met. Mater. Trans. A **29A**, 1003-1015 (1998).
[4] J.-H. Shim, Y. W. Cho, S. H. Chung, J.-D. Shim, D. N. Lee, Acta Mater. **47**, 2751-2760 (1999).
[5] H. S. Kim, H.-G. Lee, K.-S. Oh, Met. Mater. Trans. A **32A**, 1519-1525 (2001).
[6] K. Oikawa, K. Ishida, T. Nishizawa, ISIJ Int. **37**, 332-338 (1997).
[7] M. Ohta, N. Sano, K. Morita, ISIJ Int. **40**, Suppl. S87-S91 (2000).
[8] Z. Ma, D. Janke, ISIJ Intern. **38**, 46-52 (1998).
[9] M. Suzuki, R. Yamaguchi, K. Murakami, M. Nakada, ISIJ Int. **41**, 247-256 (2001).
[10] J. Wypartowicz, D. Podorska, Hutnik – Wiadomości Hutnicze **73**, 91-96 (2006).